RESEARCH ARTICLE

THE FASEB JOURNAL
The Journal of the Federation of American Societies for Experimental Biology

The chloride channel CFTR is not required for cyst growth in an ADPKD mouse model

Khaoula Talbi[1] | Inês Cabrita[1] | Andre Kraus[2] | Sascha Hofmann[1] | Kathrin Skoczynski[2] | Karl Kunzelmann[1] | Bjoern Buchholz[2] | Rainer Schreiber[1] (ORCID)

[1]Department of Physiology, University of Regensburg, Regensburg, Germany

[2]Department of Nephrology and Hypertension, Friedrich-Alexander-University Erlangen-Nuremberg, Erlangen, Germany

Correspondence
Rainer Schreiber, Department of Physiology, University of Regensburg, Universitätsstr. 31, D-93053 Regensburg, Germany.
Email: rainer.schreiber@ur.de

Abstract

Autosomal dominant polycystic kidney disease (ADPKD) is characterized by the development of bilateral renal cysts which enlarge continuously, leading to compression of adjacent intact nephrons. The growing cysts lead to a progressive decline in renal function. Cyst growth is driven by enhanced cell proliferation and chloride secretion into the cyst lumen. Chloride secretion is believed to occur mainly by the cAMP-activated cystic fibrosis transmembrane conductance regulator (CFTR), with some contribution by the calcium-activated chloride channel TMEM16A. However, our previous work suggested TMEM16A as a major factor for renal cyst formation. The contribution of CFTR to cyst formation has never been demonstrated in an adult ADPKD mouse model. We used mice with an inducible tubule-specific Pkd1 knockout, which consistently develop polycystic kidneys upon deletion of Pkd1. Cellular properties, ion currents, and cyst development in these mice were compared with that of mice carrying a co-deletion of Pkd1 and Cftr. Knockout of Cftr did not reveal any significant impact on cyst formation in the ADPKD mouse model. Furthermore, knockout of Cftr did not attenuate the largely augmented cell proliferation observed in Pkd1 knockout kidneys. Patch clamp analysis on primary renal epithelial cells lacking expression of Pkd1 indicated an only marginal contribution of CFTR to whole cell Cl⁻ currents, which were clearly dominated by calcium-activated TMEM16A currents. In conclusion, CFTR does not essentially contribute to renal cyst formation in mice caused by deletion of Pkd1. Enhanced cell proliferation and chloride secretion is caused primarily by upregulation of the calcium-activated chloride channel TMEM16A.

KEYWORDS
ADPKD, CFTR, cyst growth, proliferation, TMEM16A

1 | INTRODUCTION

Autosomal dominant polycystic kidney disease (ADPKD) is a frequent monogenic kidney disease often resulting in end-stage renal failure.[1] It is caused by mutations in either PKD1 (~85%) encoding polycystin-1 or PKD2 (~15%) encoding polycystin-2.[1] ADPKD is characterized by the development of multiple bilateral renal cysts which enlarge continuously over years and decades.[2] Continuous cyst enlargement leads to compression of adjacent intact tissue which results in decline of renal function.[2] Cyst growth is driven by increased cell proliferation and chloride transport into the cyst lumen accompanied by fluid transport secretion.[2,3]

Chloride conductance has been early demonstrated in monolayers of human ADPKD cyst cells.[4,5] Fluid secretion was stimulated by adenylyl cyclase agonists like forskolin, and also by the phosphodiesterase inhibitor 3-isobutyl-1-methylxanthine (IBMX).[6,7] The analogy between observations in ADPKD cyst epithelial cells and those in other secretory epithelial cells, suggested that cystic fibrosis transmembrane conductance regulator (CFTR) chloride channels mediate cAMP-stimulated Cl^- secretion in ADPKD cysts.[8] CFTR belongs to the ATP-binding cassette (ABC) superfamily of integral membrane transporters.[9] CFTR is regulated by cAMP-dependent phosphorylation of the regulatory (R) domain via PKA resulting in transepithelial Cl^- transport.[9] Mutations of CFTR are known to cause cystic fibrosis, a common lethal autosomal recessive disease.[10] Expression of CFTR has been detected in isolated primary ADPKD cells and ADPKD kidney extracts, with a staining pattern suggesting localization in the apical membrane of cyst-lining cells.[8]

Cl^- currents were observed in isolated ADPKD cyst cells, which were activated by forskolin or stable analogs of cAMP. These currents could be inhibited by diphenylamine-2-carboxylate, and by antisense oligonucleotide against human CFTR.[8,11] Moreover, specific inhibitors of CFTR like the thiazolidinone inhibitor CFTRinh-172, which stabilizes the channel closed state, inhibited cyst growth of MDCK cells and in cAMP-stimulated metanephric kidney cultures.[12,13] Interestingly, the CFTR inhibitors tetrazolo-CFTRinh-172 and Ph-GlyH-101 suppressed MDCK cyst enlargement without affecting cell proliferation.[12] In addition, both inhibitors retarded cyst growth in a metanephric kidney cyst model and in a neonatal, kidney-specific Pkd1 knockout (KspCre; Pkd1[flox/−]) mouse model.[12] However, the role of CFTR to polycystic kidney disease has not been demonstrated in vivo in a suitable animal model. Such a model probably reflects better the long-standing course of the disease in humans. Furthermore, a significant heterogeneity in CFTR expression has been reported in isolated primary cyst cells from ADPKD patient.[8,11,14] Notably, a milder cystic phenotype has been reported in three patients with ADPKD and cystic fibrosis, when compared to their siblings suffering from ADPKD alone.[15,16] However, the potential protective effect by cystic fibrosis in ADPKD has not been confirmed in a subsequent report.[17]

In our previous reports, we identified the calcium-activated chloride channel TMEM16A to be significantly involved in cyst growth in ADPKD.[18,19] In ADPKD, expression of TMEM16A is upregulated in the apical membrane of human cyst-lining cells.[18] Knockdown of TMEM16A (Anoctamin1; ANO1) in cyst-forming MDCK cells significantly inhibited ATP-dependent, that is, calcium-activated chloride currents.[18] ATP is released by renal epithelial cells and accumulates in the cyst fluid of human ADPKD cysts.[20,21] Pharmacological inhibition of TMEM16A and morpholinos directed against TMEM16A inhibited cyst growth in metanephric kidney cultures.[18] Importantly, tubule-specific knockout of TMEM16A as well as pharmacological inhibition by the TMEM16A inhibitors Ani9, as well as benzbromarone, and niclosamide, inhibited cyst growth in an adult Pkd1 orthologous mouse model.[19] In addition, both, knockout and inhibition of TMEM16A inhibited cyst cell proliferation markedly.[18,19] This is explained by suppression of the pro-proliferative and pro-cancerous function of TMEM16A.[22,23] The unmasked importance of TMEM16A for ADPKD asks for the proportionate contribution of CFTR to cyst formation in ADPKD. In the present study, we therefore co-deleted Cftr together with Pkd1 in adult mice, and analyzed how this would affect cyst growth, proliferation and ion currents. The data demonstrate uncompromised cyst development by deletion of CFTR. Thus, CFTR is not required for cyst formation in the examined adult ADPKD mouse model.

2 | MATERIALS AND METHODS

2.1 | Animals

Animal experiments were approved by the local institutional review board and the local Ethics Committee of the Government of Unterfranken/Wuerzburg (AZ: 55.2-2532-2-328, and AZ: 55.2.2-2532-2-853). All experiments complied with the United Kingdom Animals Act, 1986, and associated guidelines, EU Directive 2010/63/EU for animal experiments. Animals were hosted on a 12:12 h light:dark cycle under constant temperature (24 ± 1°C) in standard cages. They were fed a standard diet with free access to tap water. Generation of mice with a tamoxifen-inducible, kidney epithelium-specific Pkd1 deletion were described recently.[24] Mice carrying loxP-flanked conditional alleles of Pkd1 were crossed with KSP-Cre mice in a C57BL/6 background (KspCreER[T2]; Pkd1[lox;lox];

abbreviated as Pkd1$^{-/-}$). Mice carrying loxP-flanked Exon 10 alleles of Cftr were crossed to generate KspCreER^{T2}; Pkd1$^{lox;lox}$; Cftr$^{lox;lox}$ double knockout mice in a C57BL/6 background (abbreviated as Pkd1$^{-/-}$/Cftr$^{-/-}$). Primers for genotyping are listed in Table S1.

2.2 | Animal treatment

Conditional knockout was induced in male Pkd1$^{-/-}$ ($n = 5$) and Pkd1$^{-/-}$/Cftr$^{-/-}$ mice ($n = 7$) by intraperitoneal injection of tamoxifen (2 mg/kg body weight) dissolved in 5% ethanol and 95% neutral oil, daily at postnatal days PN 20–22. Non-induced KspCreER^{T2}; Pkd1$^{lox;lox}$ mice ($n = 5$, abbreviated as Pkd1$^{+/+}$) served as controls. All animals were sacrificed 10 weeks after induction with tamoxifen and kidneys were analyzed. In addition, and in accordance with pre-defined abort criteria, two mice were sacrificed 6 and 8 weeks after induction, respectively.

2.3 | Isolation of renal medullary primary cells

Mice were sacrificed and kidneys were removed and kept in ice-cold DMEM/F12 medium (Thermo Fisher Scientific, Darmstadt, Germany). The renal capsule was removed under germ-free conditions. Medulla was separated and chopped into smaller pieces of tissue using a sharp razor blade (Heinz Herenz, Hamburg, Germany). Tissues were incubated in Hanks balanced salt solution/DMEM/F12 (Life Technologies/Gibco, Karlsruhe, Germany) containing 1 mg/ml collagenase type 2 (Worthington, Lakewood, USA) for 20 min at 37°C. The digested tissue was passed through a 100 µm cell strainer (Merck KGaA, Darmstadt, Germany), transferred to a 50 ml falcon tube and washed with ice cold PBS. After centrifugation at 600 g for 4 min/4°C, tubules were resuspended. After washing with ice-cold PBS, tubules were maintained at 37°C/5% CO_2 in DMEM/F12 supplemented with 1% fetal bovine serum, 1% Penicillin/Streptomycin, 1% L-Glutamine (200 mM), 1% ITS (100×), 50 nM hydrocortisone, 5 nM triiodothyronine, and 5 nM epidermal growth factor (all Sigma-Aldrich, Taufkirchen, Germany). After 24 h, primary cells grew out from isolated tubules.

2.4 | RT-PCR

For RT-PCR total RNA from tissue or primary cells was isolated using NucleoSpin RNA II columns (Macherey-Nagel, Dueren, Germany). Total RNA (1 µg/50 µl reaction) was reverse transcribed using random primer (Promega, Mannheim, Germany) and M-MLV Reverse Transcriptase RNase H Minus (Promega). Each RT-PCR reaction contained sense (0.5 µM) and antisense primer (0.5 µM) (Table S2), 0.5 µl cDNA and GoTaq Polymerase (Promega). After 2 min at 95°C cDNA was amplified (35 cycles for target sequence and 30 cycles for the reference GAPDH) for 30 s at 95°C, 30 s at 56°C and 1 min at 72°C. PCR products were visualized by loading on peqGREEN (Peqlab; Duesseldorf, Germany) containing agarose gels and analyzed using ImageJ.

2.5 | Western Blotting

2.5.1 | Isolated medullary renal primary cells

Proteins were isolated using a sample buffer containing 25 mM Tris-HCl, 150 mM NaCl, 100 mM dithiothreitol, 5.5% Nonidet P-40, 5% glycerol, 1 mM EDTA, and 1% protease inhibitor mixture (Roche, cOmplete, EDTA-free, Mannheim, Germany). Proteins were separated by 8.5% sodium dodecyl sulfate (SDS) polyacrylamide gel and transferred to a polyvinylidene difluoride membrane (GE Healthcare Europe GmbH, Munich, Germany) or 4%–20% Mini-PROTEAN TGX Stain-Free (Bio-Rad) using a semi-dry transfer unit (Bio-Rad, Hercules, CA, USA). Membranes were incubated with primary anti-TMEM16A rabbit polyclonal antibody (Davids Biotech, Regensburg, Germany; 1:1000), anti-CFTR (alomone labs, Jerusalem, Israel, 1:1000), or anti-PKD1 (Polycystin-1 (7E12), Santa Cruz; 1:500) mouse antibody overnight at 4°C. Proteins were visualized using horseradish peroxidase-conjugated secondary antibody and ECL detection. Beta-Actin was used as a loading control. *Whole kidneys:* Proteins were isolated using a sample buffer containing 50 mM Tris-HCl, 150 mM NaCl, 10 mM EDTA, 1% sodium deoxycholate, 0.1% SDS and 1% protease inhibitor mixture (Roche, cOmplete, EDTA-free), and 1% Triton X-100. Proteins were separated using 8% SDS polyacrylamide gels for TMEM16A and NuPAGE 3%–8% Tris-Acetate Protein Gels for CFTR (Life Technologies/Gibco). For detection of TMEM16A the proteins were blotted via iBlot 2 Dry Blotting System (Thermo Fisher Scientific) to a polyvinylidene difluoride membrane (GE Healthcare Europe GmbH, Munich, Germany). For detection of CFTR the proteins were blotted using a semi-dry transfer unit (Bio-Rad) for 3 h. The membranes were incubated with primary antibody anti-TMEM16A DOG-1 polyclonal (Thermo Fisher, 1:1000) and anti-CFTR (Alomone labs, Jerusalem, Israel 1:500) overnight at 4°C. Proteins were visualized using horseradish peroxidase-conjugated secondary antibody and ECL detection. Beta-Actin was used as loading control.

2.6 | Immunohistochemistry and antibodies

Affinity purified polyclonal antiserum against mouse TMEM16A was produced in rabbits immunized with DPDAECKYGLYFRDGKRKVD (aa 44-63, N-terminus) or NHSPTTHPEAGDGSPVPSYE (aa 957-976, C-terminus), coupled to keyhole limpet hemocyanin (Davids Biotechnologie, Regensburg, Germany) as described previously.[18] Mouse kidneys were fixed by perfusion with 4% (v/v) paraformaldehyde and post-fixed in 0.5 mol/L sucrose and 4%
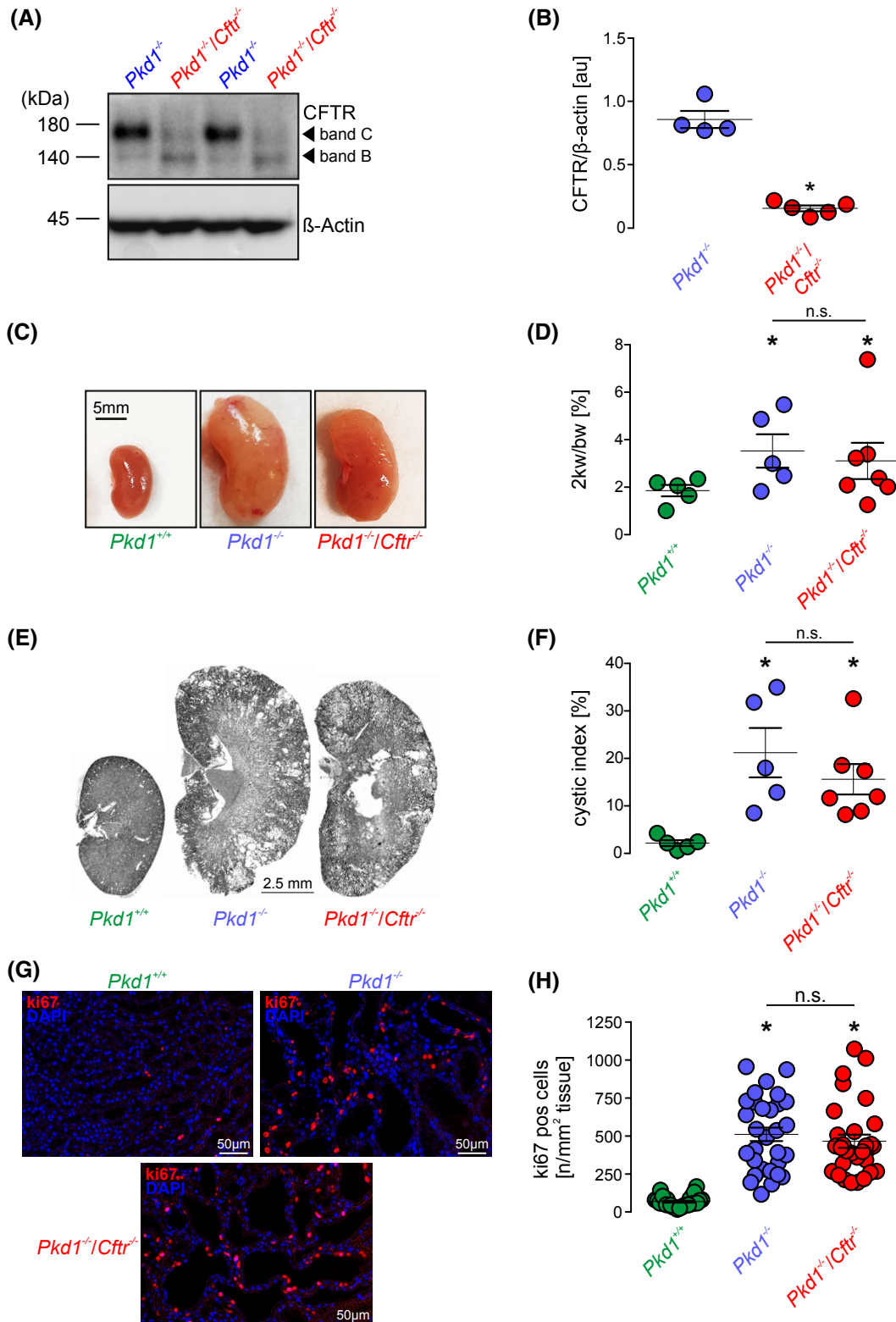
paraformaldehyde solution. Paraffin sections of 2 μm were blocked with 5% bovine serum albumin (BSA) and 0.04% Triton X-100 in PBS for 30 min. For co-staining of CFTR and TMEM16A, anti-CFTR (rabbit; 1:100; Alomone labs) and anti-TMEM16A (rabbit; 1:200, P80, described previously[19]) antibodies were used in 0.5% BSA and 0.04% Triton X-100 overnight at 4°C. As secondary antibodies, anti-rabbit IgG Alexa Fluor 555 and 488 antibodies (1:1000; Thermo Fisher Scientific) were used. Ki-67 staining was performed using a monoclonal anti-ki-67 antibody (rabbit; 1:100, Linaris, Dossenheim, Germany). Sections were counterstained with Hoe33342 (1:200, Sigma-Aldrich). Signals were amplified by the use of the Vectastain Elite ABC Kit (Vector Laboratories, Burlingame, CA) according to the manufacturer′s instructions. Signals were analyzed with a DM6000B fluorescence microscope (Leica, Wetzlar, Germany), and photographs were taken with a Leica DFC 450C camera.

2.7 | Quantification of immunohistochemistry and fluorescent signals

Four random photographs were taken from the cortex of each kidney ($n = 5$ per condition) at a magnification of X200. Immunofluorescence (TMEM16A and CFTR) was analyzed as described previously.[19] Briefly, fluorescent signals were turned into 8-bit images after subtracting background (ImageJ) and a predefined threshold was used for all images to capture signals. For quantification of ki67, the color deconvolution algorithm (ImageJ) was applied to dissect the different signals, followed by binarization and particle analysis to obtain the ratio of the number of positive cells and cortex area (normalized to mm^2 cortex tissue).

2.8 | Morphological analyses

Photographs from hematoxylin and eosin-stained kidney sections were taken at a magnification of X25 and stitched to obtain single photographs of the whole transverse kidney sections using a Leica DM6000B microscope and a Leica DFC 450C camera. We used an algorithm that separates normal tubule space from cystic area by defining diameters of non-cystic tubules <50 μm (ImageJ) as described previously.[24] The whole cyst area was divided by the whole cortex area and defined as cystic index.

2.9 | YFP-quenching assay

For YFP-quenching assays, primary renal cells were infected with lentiviral vectors to express halide-sensitive YFP$_{I152L}$, as previously described.[25] Cells were isolated from four different mice per condition and for each mouse 40 cells were measured. Quenching of the intracellular fluorescence generated by the iodide sensitive Enhanced Yellow Fluorescent Protein (EYFP-I152L) was used to measure anion conductance. YFP-I152L fluorescence was excited at 500 nm using a polychromatic illumination system for microscopic fluorescence measurement (Visitron Systems, Puchheim, Germany) and the emitted light measured at 535 $\pm$ 15 nm with a Coolsnap HQ CCD camera (Roper Scientific). Cells were grown on cover slips and mounted in a thermostatically controlled imaging chamber maintained at 37°C. Cells were continuously perfused at 8 ml/min with Ringer solution (mmol/l: NaCl 145; KH$_2$PO$_4$ 0.4; K$_2$HPO$_4$ 1,6; Glucose 5; MgCl$_2$ 1; Ca^{2+}-gluconate 1.3) and quenching of YFP-I152L fluorescence by I$^-$ influx was induced by replacing 5 mM extracellular Cl$^-$ with I$^-$ and exposed to I$^-$ concentration of 5 mM by replacing same amount of NaCl with equimolar NaI. Background

FIGURE 1 Knockout of Cftr does not inhibit cyst development in ADPKD. Tubule-specific knockout of Pkd1 (Pkd1$^{-/-}$) or double knockout of Pkd1 and Cftr (Pkd1$^{-/-}$/CFTR$^{-/-}$) was induced by application of tamoxifen at postnatal day 20–22. Non-induced KspCreER^{T2}; Pkd1$^{lox;lox}$ mice served as control (Pkd1$^{+/+}$). Analyses were performed 10 weeks after induction. (A) Western blotting from whole kidney lysates from Pkd1$^{-/-}$ ($n = 4$), and Pkd1$^{-/-}$/Cftr$^{-/-}$ ($n = 5$) mice detecting reduced expression of CFTR. The core glycosylated immature form of CFTR is designated as "band B." The complex glycosylated form of CFTR, representing transit through the Golgi, is termed "band C." (B) Quantification of expression of CFTR based on densitometric analysis with CFTR (band C) normalized to β-actin. *Significant difference when compared to Pkd1$^{-/-}$, t test. (C) Tubule-specific knockout of Pkd1 (Pkd1$^{-/-}$; $n = 5$ animals) induced polycystic kidney disease indicated by increased kidney weight. Additional knockout of Cftr (Pkd1$^{-/-}$/Cftr$^{-/-}$; $n = 7$ animals) did not prevent cyst formation and kidney weight. Non-induced KspCreER^{T2}; Pkd1$^{lox;lox}$ (Pkd1$^{+/+}$; $n = 5$ animals) served as controls. (D) Summary of two times kidney weight (2 kw) to body weight (bw). *Significant difference when compared to Pkd1$^{+/+}$, one-way ANOVA, Posthoc test: Bonferroni–Holm. (E) Tubule-specific knockout of Pkd1 (Pkd1$^{-/-}$; $n = 5$ animals) induced cyst formation. Additional knockout of Cftr (Pkd1$^{-/-}$/Cftr$^{-/-}$; $n = 7$ animals) did not prevent cyst formation. Non-induced KspCreER^{T2}; Pkd1$^{lox;lox}$ (Pkd1$^{+/+}$; $n = 5$ animals) served as controls. (F) Corresponding cystic indices (defined as cortical cyst area normalized to whole cortex area). Mean $\pm$ SEM. *Significant difference when compared to Pkd1$^{+/+}$, one-way ANOVA, Posthoc test: Bonferroni–Holm. (G) Analysis of cell proliferation in Pkd1$^{+/+}$, Pkd1$^{-/-}$, and Pkd1$^{-/-}$/Cftr$^{-/-}$ tissues indicated by Ki67 expression. (H) Summary of Ki67 positive cells/mm^2 tissue area in Pkd1$^{+/+}$, Pkd1$^{-/-}$, and Pkd1$^{-/-}$/Cftr$^{-/-}$ kidneys. Mean $\pm$ SEM. *Significant difference when compared to Pkd1$^{+/+}$, one-way ANOVA, Posthoc test: Bonferroni–Holm
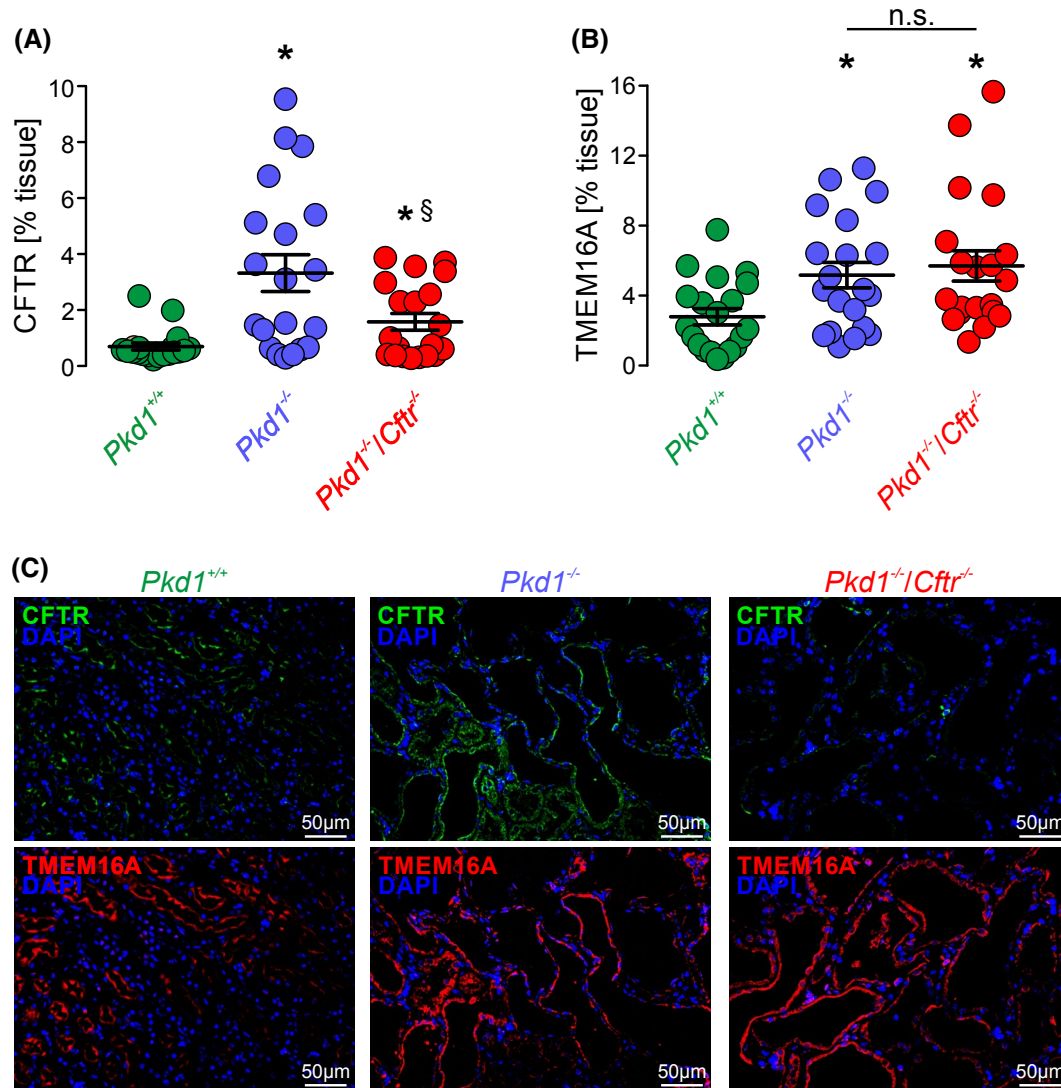
FIGURE 2 TMEM16A is upregulated in Pkd1$^{-/-}$ as well as in Pkd1$^{-/-}$/Cftr$^{-/-}$ double-knockout animals. Kidney sections from Pkd1$^{+/+}$, Pkd1$^{-/-}$, Pkd1$^{-/-}$/CFTR$^{-/-}$ mice (each $n = 5$ animals with each a total of $n = 20$ photos) were stained for CFTR and TMEM16A. (A) Analysis of CFTR-positive area in relation to the whole cortex area. (B) Analysis of TMEM16A-positive area in relation to the whole cortex area. *Significant difference when compared to Pkd1$^{+/+}$, unpaired t test. §Significant difference when compared to Pkd1$^{-/-}$, one-way ANOVA, Posthoc test: Bonferroni–Holm. (C) Representative CFTR stainings (green) and nuclei (blue) in the upper panel and representative TMEM16A stainings (red) and nuclei (blue) in the lower panel

fluorescence was subtracted, while auto-fluorescence was negligible. Changes in fluorescence induced by I^{-} are expressed as initial rates of maximal fluorescence decrease ($\Delta F/\Delta t$). For quantitative analysis, cells with low or excessively high fluorescence were discarded.

2.10 | Patch clamping

Patch clamp experiments were performed in the fast whole-cell configuration. Patch pipettes had an input resistance of 2–4 MΩ, when filled with a solution containing (mM) KCl 30, K^{+}-gluconate 95, NaH$_2$PO$_4$ 1.2, Na$_2$HPO$_4$ 4.8, EGTA

1, Ca^{2+}-gluconate 0.758, MgCl$_2$ 1.034, D-glucose 5, ATP 3. pH was 7.2, the Ca^{2+} activity was 0.1 μM. The access conductance was measured continuously and was 30–140 nS. Currents (voltage clamp) and voltages (current clamp) were recorded using a patch clamp amplifier (EPC 7, List Medical Electronics, Darmstadt, Germany), the LIH1600 interface and PULSE software (HEKA, Lambrecht, Germany) as well as Chart software (AD-Instruments, Spechbach, Germany). Data were stored continuously on a computer hard disc and were analyzed using PULSE software. In regular intervals, membrane voltages (V_c) were clamped in steps of 20 mV from −100 to +100 mV relative to resting potential. Membrane conductance G_m was

(A)

con   IF
Pkd1⁺/⁺

con   IF
Pkd1⁻/⁻

con   IF
Pkd1⁻/⁻/Cftr⁻/⁻

(B)

Pkd1⁺/⁺

Pkd1⁻/⁻

Pkd1⁻/⁻/Cftr⁻/⁻

(C)
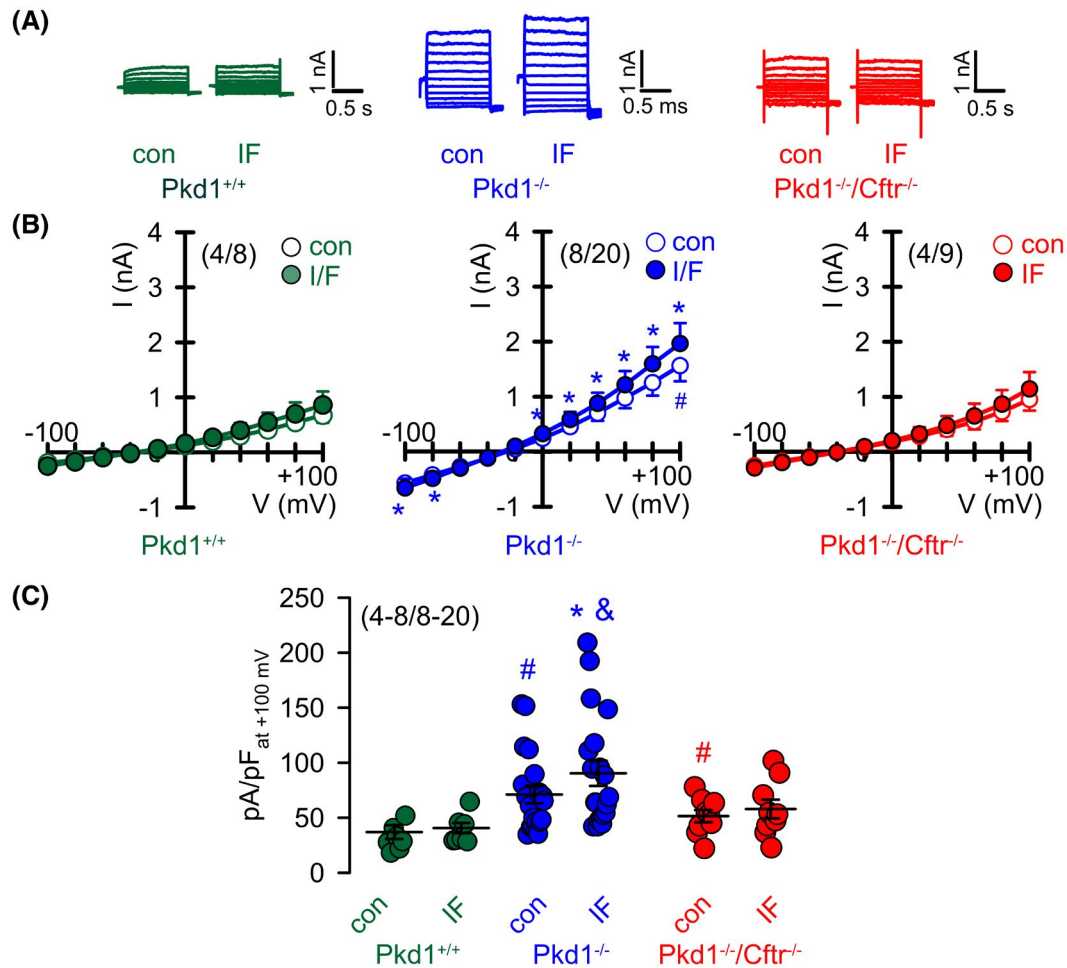
FIGURE 3 cAMP-activated CFTR currents make a minor contribution to the whole cell Cl⁻ conductance in Pkd1⁻/⁻ cells. Whole cell patch clamp recordings in primary epithelial cells from Pkd1⁺/⁺, Pkd1⁻/⁻, and Pkd1⁻/⁻/Cftr⁻/⁻ mice were performed. Currents were obtained under basal conditions (Con) and after stimulation with IBMX/Forskolin (IF, 100 μM/2 μM). (A) Original whole cell patch clamp recordings in primary epithelial cells from Pkd1⁺/⁺, Pkd1⁻/⁻, and Pkd1⁻/⁻/Cftr⁻/⁻ mice showing currents obtained under basal conditions and after stimulation with IF. (B) I/V curves for the currents shown in A. (C) Summaries of the current densities for the currents summarized in I/V curves shown in B. (number of mice/number of cells). *Significant difference when compared to control, paired t test. #Significant difference when compared to Pkd1⁺/⁺ con, and significant difference when compared to Pkd1⁺/⁺ IF, one-way ANOVA, Posthoc test: Bonferroni–Holm

calculated from the measured current (I) and V_c values according to Ohm's law.

2.11 | Statistics

Data are reported as mean ± SEM. Student's t test for unpaired samples and ANOVA were used for statistical analysis. A p value of <.05 was accepted as significant difference. Data are expressed as mean ± SEM. Differences among groups were analyzed using one-way ANOVA, followed by a Bonferroni test for multiple comparisons. An unpaired or paired t test was applied to compare the differences between two groups. $p < .05$ was considered statistically significant.

3 | RESULTS

3.1 | Knockout of Cftr does not inhibit cyst development in ADPKD mice

Pkd1 knockout was achieved by tamoxifen treatment at postnatal day 20–22 of KspCreER^T2; Pkd1^lox;lox and KspCreER^T2; Pkd1^lox;lox/Cftr^lox;lox animals to generate either single tubule-specific Pkd1⁻/⁻ knockout or double Pkd1⁻/⁻/Cftr⁻/⁻ knockout animals (Figure 1A,B). Knockout of Pkd1 led to a significant polycystic kidney phenotype 10 weeks after induction (Figure 1C,D). Remarkably, additional knockout of Cftr had no impact on cyst formation (Figure 1C,D). As reported previously, knockout of Pkd1 enhanced renal cell proliferation
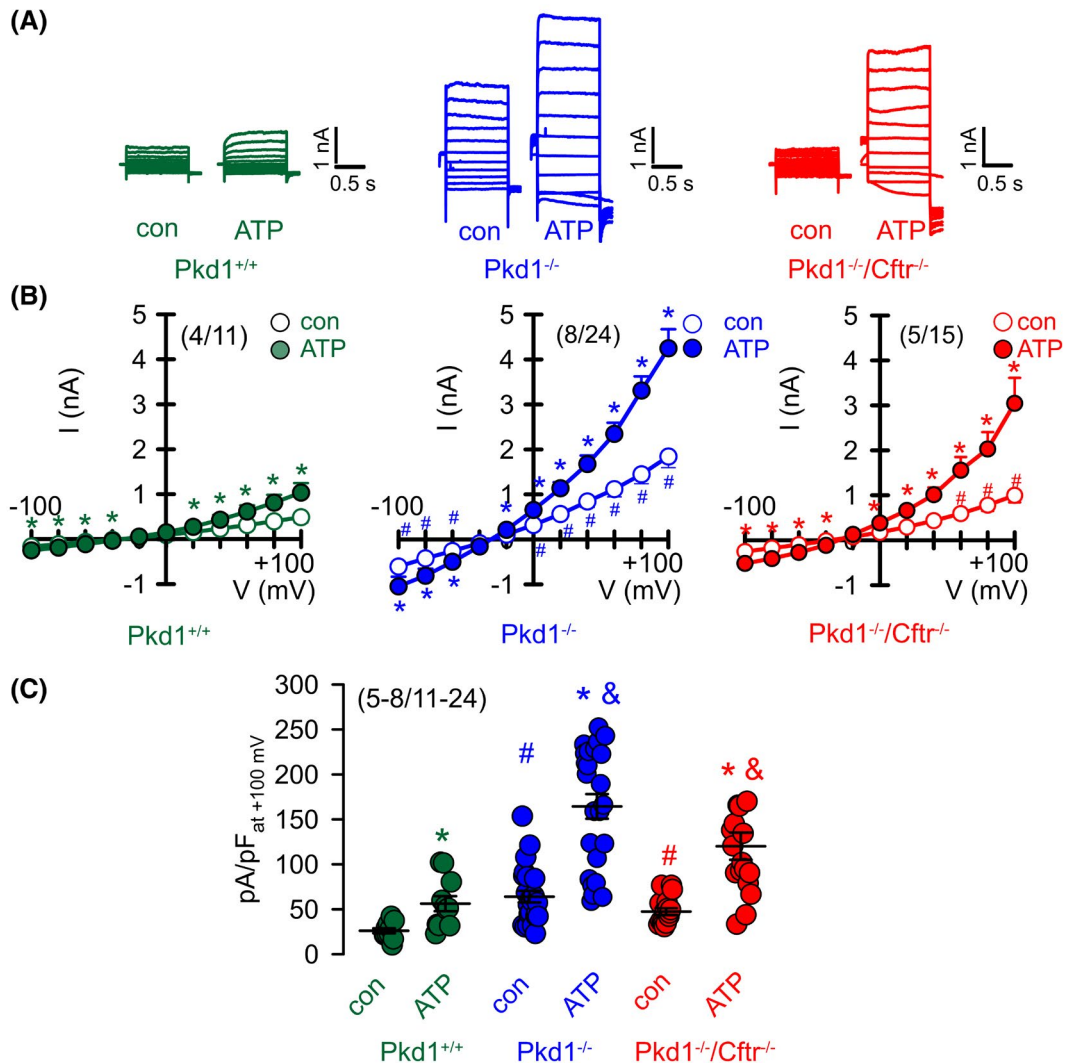
FIGURE 4 Ca^{2+}-activated Cl^- currents are upregulated in $Pkd1^{-/-}$ cells independent of CFTR expression. Whole cell patch clamp recordings in primary epithelial cells from $Pkd1^{+/+}$, $Pkd1^{-/-}$, and $Pkd1^{-/-}/Cftr^{-/-}$ mice were performed. Currents were obtained under basal conditions (Con) and after stimulation with ATP (50 μM). (A) Original whole cell patch clamp recordings in primary epithelial cells from $Pkd1^{+/+}$, $Pkd1^{-/-}$, and $Pkd1^{-/-}/Cftr^{-/-}$ mice illustrating currents obtained under basal conditions and after stimulation with ATP. (B) I/V curves for the currents shown in A. (C) Summaries of the current densities for the currents summarized in I/V curves shown in B. (number of mice/number of cells). *Significant difference when compared to control, paired t test. #Significant difference when compared to $Pkd1^{+/+}$ con, and significant difference when compared to $Pkd1^{+/+}$ cells stimulated with ATP, one-way ANOVA, Posthoc test: Bonferroni–Holm

significantly (Figure 1E,F).[19] This increase in cell proliferation was unaffected by additional knockout of Cftr (Figure 1E,F). These data indicate that CFTR is not required for upregulation of proliferation and cyst growth in adult ADPKD mice.

## 3.2 | TMEM16A is upregulated in $Pkd1^{-/-}$ mice, independent of CFTR

Knockout of Pkd1 causes upregulation of TMEM16A in kidneys of mouse and human.[19,26] Upregulation of TMEM16A expression and ATP-activated whole cell

currents persist throughout disease development and increase over time (Figure S1). In kidneys from $Pkd1^{-/-}$ mice, enhanced expression of TMEM16A is detected in the apical membrane of the cyst epithelium, along with upregulation of CFTR (Figure 2). Due to the relationship of CFTR and TMEM16A reported earlier,[19,27] we wondered whether deletion of CFTR would affect expression of TMEM16A. However, in the absence of CFTR, TMEM16A expression was still found to be enhanced by deletion of Pkd1 (Figure 2). Western blots from whole kidney lysates indicate that loss of CFTR expression in $Pkd1^{-/-}/Cftr^{-/-}$ kidneys does not affect expression of TMEM16A (Figure S2).
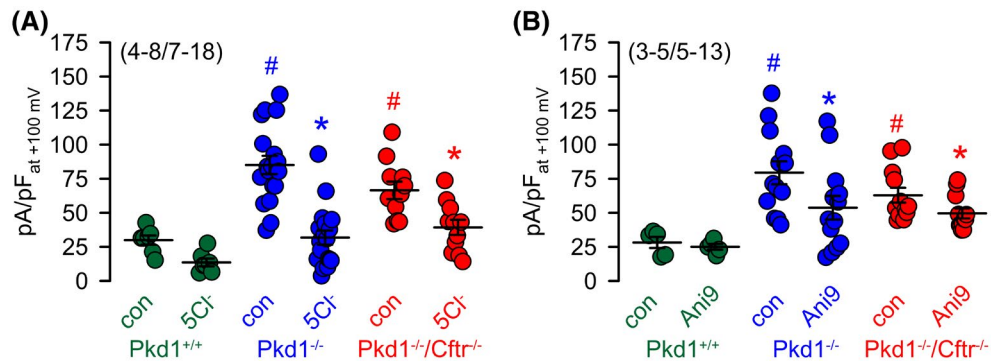
FIGURE 5 Ca^{2+}-activated Cl^- currents dominate in $Pkd1^{-/-}$ cells and are mediated by TMEM16A. Whole cell patch clamp recordings in primary epithelial cells from $Pkd1^{+/+}$, $Pkd1^{-/-}$, and $Pkd1^{-/-}/Cftr^{-/-}$ mice were performed. Currents were obtained under basal conditions (Con), after removal of extracellular Cl^- by replacement with the impermeable gluconate ions (5 Cl^-), or in the presence of 10 μM of the TMEM16A inhibitor Ani9. (A) Summaries for current densities under basal conditions (Con) and after Cl^- removal (5 Cl^-). (B) Summaries for current densities under basal conditions and after application of the TMEM16A inhibitor Ani9. (number of mice/number of cells). *Significant difference when compared to control, paired t test. #Significant difference when compared to $Pkd1^{+/+}$ con, one-way ANOVA, Posthoc test: Bonferroni–Holm
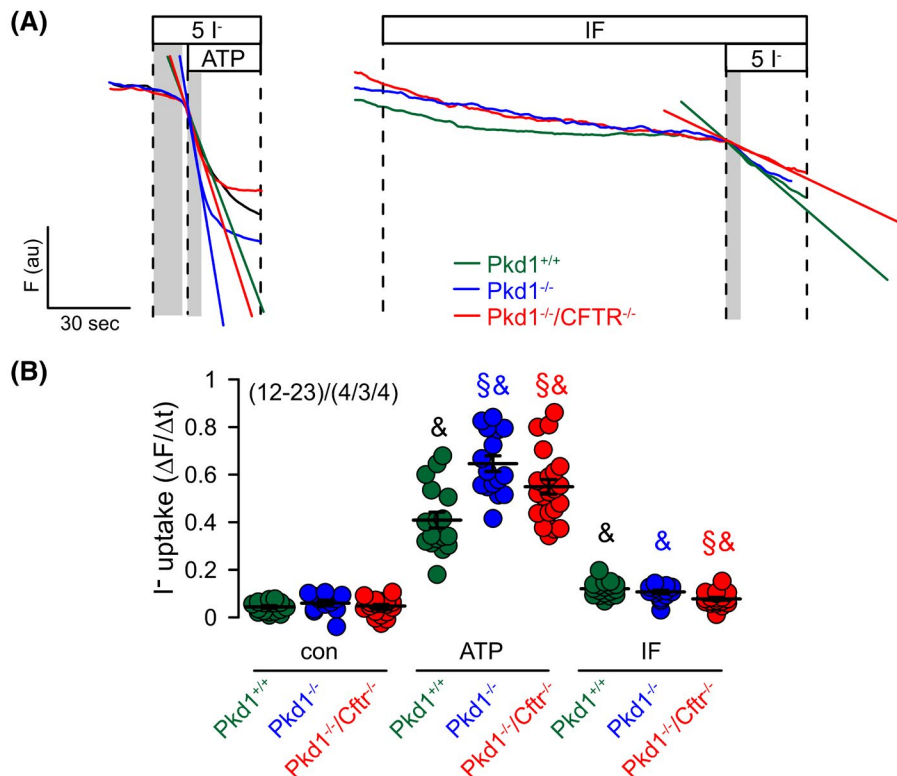
FIGURE 6 Halide permeability in $Pkd1^{-/-}$ cells largely depends on Ca^{2+}- but not cAMP-mediated signaling. Measurement of iodide-induced quenching of yellow fluorescent protein (YFP) in isolated primary renal epithelial cells from $Pkd1^{+/+}$, $Pkd1^{-/-}$, and $Pkd1^{-/-}/Cftr^{-/-}$ mice were performed in the presence of 5 mM extracellular iodide (5 I^-) under basal conditions (Con), in the presence of ATP (100 μM), or in the presence of IBMX/Forskolin (IF, 100 μM/2 μM). (A) Original tracings for basal, Ca^{2+}- and IF-activated (100 μM ATP) anion conductances detected by YFP quenching in cells from $Pkd1^{+/+}$, $Pkd1^{-/-}$, and $Pkd1^{-/-}/Cftr^{-/-}$ mice. To measure the fast activation of iodide conductance by ATP, ATP was added in the presence of iodide. However, iodide was added after 2 min IF incubation when iodide conductance was maximal (determinate by patch clamp experiments). Initial slopes correlate with the size of anion conductance. (B) Summary of initial slopes (ΔFluorescence/s) for the experiments shown in A. (number of mice/number of measured cells). §Significant difference when compared to $Pkd1^{+/+}$, one-way ANOVA, Posthoc test: Bonferroni–Holm. &Significant difference when compared to control (con), one-way ANOVA, Posthoc test: Bonferroni–Holm, $Significant difference to $Pkd1^{+/+}$ IF and $Pkd1^{-/-}$ IF one-way ANOVA, Posthoc test: Bonferroni–Holm

3.3 | Dominating TMEM16A currents in renal epithelial cells from Pkd1$^{-/-}$ mice

The above-mentioned results ask for the contribution of CFTR to the chloride currents present in primary renal epithelial cells. Therefore, medullary renal primary cells were isolated and characterized 8–10 weeks after induction confirming distal tubular origin of the cells (Figure S3). Of note, and in line with previous findings,[24,28] Pkd1 knockout resulted in an increased expression of the purinergic receptor P2y2 (Figure S3). Increase in intracellular cAMP by IBMX (100 μM) and forskolin (2 μM) (I/F) activated no CFTR-mediated whole cell currents in Pkd1-competent cells (Figure 3). We demonstrated earlier that loss of Pkd1 leads to upregulation of CFTR expression.[19] In fact, a small but significant I/F-activated CFTR current was observed in renal cells isolated from Pkd1$^{-/-}$ animals, which was abolished by additional knockout of Cftr (Figure 3). Expression of CFTR in Pkd1$^{-/-}$ mice as well as depletion of CFTR in Pkd1$^{-/-}$/Cftr$^{-/-}$ mice has been confirmed by Western blotting of whole kidney lysates (Figure S2) and isolated primary epithelial cells (Figure S4). In contrast to the small CFTR-mediated whole cell current, the ATP-activated TMEM16A-dependent current was much more prominent in Pkd1$^{-/-}$ cells, and was not attenuated by additional knockout of Cftr (Figure 4). These results correspond well to previous findings reported in mouse primary medullary epithelial cells and M1 mouse collecting duct cells lacking expression of Pkd1.[19,29] The present data also suggest enhanced basal membrane currents in PKD1$^{-/-}$ cells in the absence of ATP (Figures 4 and 5). Enhanced currents are not detectable when related to the membrane surface area (current density, pA/pF) presumably because of the larger cell size and capacitance of Pkd1$^{-/-}$ cells due to loss of polycystin-1.[30] Removal of extracellular chloride or current inhibition by the TMEM16A-inhibitor Ani9 indicated a basal activity of TMEM16A in PKD1$^{-/-}$ cells (Figure 5).

In order to validate enhanced ATP-activated chloride currents in Pkd1$^{-/-}$ and Pkd1$^{-/-}$/Cftr$^{-/-}$ cells, we used an independent technique to assess the anion permeability by measuring iodide-induced quenching of yellow fluorescent protein (YFP). In the presence of 5 mM iodide (5 I$^-$) in the extracellular bath solution, stimulation with ATP (100 μM) caused a rapid YFP-fluorescence quenching. ATP-induced quenching was enhanced in both Pkd1$^{-/-}$ and Pkd1$^{-/-}$/Cftr$^{-/-}$ cells, thus confirming the results obtained in patch clamp experiments (Figure 6). I/F (cAMP increase) activated a small but significant YFP quenching in Pkd1$^{-/-}$ but not Pkd1$^{+/+}$ and Pkd1$^{-/-}$/Cftr$^{-/-}$ cells, which again shows a minimal contribution of CFTR to chloride secretion by renal epithelial cells from mice lacking PKD1.

Our results demonstrate that renal cyst formation in an adult mouse ADPKD model is largely independent of CFTR. In connection with our previous report we conclude that inhibition of TMEM16A[18,19,29] rather than CFTR[12,31] will be effective to reduce cyst growth in ADPKD.

4 | DISCUSSION

Cyst growth in ADPKD is mediated by chloride secretion and fluid transport across the cyst epithelium into the cyst lumen. The chloride channel CFTR has been suggested to be largely involved in this process based on numerous findings in MDCK cells, human ADPKD cyst cells, cAMP-stimulated metanephric mouse kidneys, and a neonatal, kidney-specific Pkd1 knockout mouse model (reviewed in Ref. [3]). In contrast, we show that knockout of Cftr in an adult Pkd1 orthologous mouse model does not inhibit cyst formation. CFTR currents activated by cAMP (I/F) only slightly contributed to whole cell currents in primary renal epithelial cells isolated from Pkd1$^{-/-}$ knockout mice. Instead, we found that knockout of Pkd1 resulted in enhanced expression of TMEM16A, causing pronounced ATP-dependent, that is, calcium-activated chloride currents in Pkd1$^{-/-}$ cells, and, importantly, also in Pkd1$^{-/-}$/Cftr$^{-/-}$ cells. This is seemingly in contradiction with earlier in vitro studies.[4,6] In other studies with primary cells from ADPKD patients, ATP-dependent chloride transport strongly assisted cAMP-dependent chloride currents.[32,33] These data are in line with our own studies showing a pronounced crosstalk between cAMP- and calcium-dependent signaling pathways: (i) purinergic receptors such as P2Y2R increase intracellular calcium. (ii) Intracellular calcium affects the activity of enzymes that control intracellular cAMP like adenylate cyclases.[27,34] (iii) Intracellular cAMP and PKA affect proteins like SERCA which in contrast affects intracellular calcium levels. (iv) Most importantly, membrane expression of CFTR requires the presence of TMEM16A.[27,35] Tubular deletion of TMEM16A in our Pkd1 orthologous model was accompanied by significant reduction of CFTR expression.[19] In vivo renal cyst development largely depends on enhanced cell proliferation and on TMEM16A-mediated fluid secretion, apart from additional reported factors.[19,29] For both, cell proliferation and fluid secretion, upregulation of TMEM16A expression is largely responsible, while CFTR does not contribute to augmented cell proliferation in Pkd1$^{-/-}$ kidneys. Upregulation of TMEM16A enhances cyclin D1 and the MAPK kinase pathway.[36] Moreover, cyclin kinase D1 (CDK1) was found to be dysregulated in Pkd1 orthologous mouse models.[37] Conditional co-deletion of CDK1 significantly improved progression of the disease.[37]

Appearance of TMEM16A currents and a small but significant CFTR current in renal primary cells, required the

knockout of Pkd1. It was not observed in control cells, making a culture artifact unlikely. Moreover, the role of TMEM16A for chloride transport has now been demonstrated by patch clamping, YFP quenching, and Ussing chamber measurements. We chose a mouse model with a time-course of 10 weeks resulting in polycystic kidneys, which, however, still was not lethal and did not result in decline of renal function as shown previously.[24] This model, although being still rather rapid compared to the course of the disease in humans, may better reflect disease progression found in humans than embryonic ex vivo or neonatal in vivo cyst development occurring within a few days. Of note, CFTR may play a more prominent role in neonatal or embryonic tubule cells which would explain the significant impact of CFTR in early onset and rapid progressive PKD models.[12,13] Kidneys in our mouse model experience hypoxia upon expanding cyst enlargement, which leads to induction of the hypoxia-inducible transcription factor (HIF)-1α.[24] This further promotes calcium-activated chloride secretion, for example, by transcriptional induction of P2Y2R.[24,28,38] Activation of HIF-1α might vary between the different models, which may determine the contribution of CFTR and TMEM16A.

After all, we did find a small but significant CFTR-mediated chloride secretion. Such an ongoing secretion that takes place over years in human disease, may have an impact on disease progression in patients. At last it should be mentioned that the contribution of CFTR to epithelial chloride secretion is variable in the mouse, with lower activity in the airways but pronounced contribution in the intestine.[39–41] Apart from a few findings, loss of CFTR function does not lead to an overt phenotype in human and mouse. A more recent report shows that in healthy mice it is only expressed in ß-intercalated cells, where it controls bicarbonate secretion.[42]

Taken together the present data together with previous reports[18,19,29] identify TMEM16A rather than CFTR as a promising pharmacological target to inhibit cyst growth in ADPKD.

DISCLOSURES
BB has received lecture fees from Otsuka Pharmaceutical. All other authors declared no competing interests.

AUTHOR CONTRIBUTIONS
Karl Kunzelmann, Bjoern Buchholz, and Rainer Schreiber designed the research. Inês Cabrita, Andre Kraus, Sascha Hofmann, and Kathrin Skoczynski performed the research. Karl Kunzelmann, Bjoern Buchholz, and Rainer Schreiber wrote the paper. All authors analyzed the data.

ORCID
Rainer Schreiber https://orcid.org/0000-0002-3974-5363

REFERENCES
1. Torres VE, Harris PC, Pirson Y. Autosomal dominant polycystic kidney disease. *Lancet*. 2007;369(9569):1287-1301.
2. Grantham JJ, Mulamalla S, Swenson-Fields KI. Why kidneys fail in autosomal dominant polycystic kidney disease. *Nat Rev Nephrol*. 2011;7(10):556-566.
3. Terryn S, Ho A, Beauwens R, Devuyst O. Fluid transport and cystogenesis in autosomal dominant polycystic kidney disease. *Biochem Biophys Acta*. 2011;1812(10):1314-1321.
4. Grantham JJ, Ye M, Gattone VH 2nd, Sullivan LP. In vitro fluid secretion by epithelium from polycystic kidneys. *J Clin Investig*. 1995;95(1):195-202.
5. Ye M, Grantham JJ. The secretion of fluid by renal cysts from patients with autosomal dominant polycystic kidney disease. *N Engl J Med*. 1993;329(5):310-313.
6. Mangoo-Karim R, Ye M, Wallace DP, Grantham JJ, Sullivan LP. Anion secretion drives fluid secretion by monolayers of cultured human polycystic cells. *Am J Physiol*. 1995;269(3 pt 2):F381-F388.
7. Wallace DP, Grantham JJ, Sullivan LP. Chloride and fluid secretion by cultured human polycystic kidney cells. *Kidney Int*. 1996;50(4):1327-1336.
8. Hanaoka K, Devuyst O, Schwiebert EM, Wilson PD, Guggino WB. A role for CFTR in human autosomal dominant polycystic kidney disease. *Am J Physiol*. 1996;270(1 pt 1):C389-C399.
9. Gadsby DC, Vergani P, Csanády L. The ABC protein turned chloride channel whose failure causes cystic fibrosis. *Nature*. 2006;440(7083):477-483.
10. Ratjen F, Döring G. Cystic fibrosis. *Lancet*. 2003;361(9358):681-689.
11. Davidow CJ, Maser RL, Rome LA, Calvet JP, Grantham JJ. The cystic fibrosis transmembrane conductance regulator mediates transepithelial fluid secretion by human autosomal dominant polycystic kidney disease epithelium in vitro. *Kidney Int*. 1996;50(1):208-218.
12. Yang B, Sonawane ND, Zhao D, Somlo S, Verkman AS. Small-molecule CFTR inhibitors slow cyst growth in polycystic kidney disease. *J Am Soc Nephrol*. 2008;19(7):1300-1310.

13. Magenheimer BS, St John PL, Isom KS, et al. Early embryonic renal tubules of wild-type and polycystic kidney disease kidneys respond to cAMP stimulation with cystic fibrosis transmembrane conductance regulator/Na(+), K(+),2Cl(-) Co-transporter-dependent cystic dilation. *J Am Soc Nephrol*. 2006;17(12):3424-3437.

14. Brill SR, Ross KE, Davidow CJ, Ye M, Grantham JJ, Caplan MJ. Immunolocalization of ion transport proteins in human autosomal dominant polycystic kidney epithelial cells. *Proc Natl Acad Sci USA*. 1996;93(19):10206-10211.

15. O'Sullivan DA, Torres VE, Gabow PA, Thibodeau SN, King BF, Bergstralh EJ. Cystic fibrosis and the phenotypic expression of autosomal dominant polycystic kidney disease. *Am J Kidney Dis*. 1998;32(6):976-983.

16. Xu N, Glockner JF, Rossetti S, Babovich-Vuksanovic D, Harris PC, Torres VE. Autosomal dominant polycystic kidney disease coexisting with cystic fibrosis. *J Nephrol*. 2006;19(4):529-534.

17. Persu A, Devuyst O, Lannoy N, et al. CF gene and cystic fibrosis transmembrane conductance regulator expression in autosomal dominant polycystic kidney disease. *J Am Soc Nephrol*. 2000;11(12):2285-2296.

18. Buchholz B, Faria D, Schley G, Schreiber R, Eckardt KU, Kunzelmann K. Anoctamin 1 induces calcium-activated chloride secretion and proliferation of renal cyst-forming epithelial cells. *Kidney Int*. 2014;85(5):1058-1067.

19. Cabrita I, Kraus A, Scholz JK, et al. Cyst growth in ADPKD is prevented by pharmacological and genetic inhibition of TMEM16A in vivo. *Nat Commun*. 2020;11(1):4320.

20. Wilson PD, Hovater JS, Casey CC, Fortenberry JA, Schwiebert EM. ATP release mechanisms in primary cultures of epithelia derived from the cysts of polycystic kidneys. *J Am Soc Nephrol*. 1999;10(2):218-229.

21. Praetorius HA, Leipziger J. ATP release from non-excitable cells. *Purinergic Signal*. 2009;5(4):433-446.

22. Chênevert J, Duvvuri U, Chiosea S, et al. DOG1: a novel marker of salivary acinar and intercalated duct differentiation. *Mod Pathol*. 2012;25(7):919-929.

23. Ruiz C, Martins JR, Rudin F, et al. Enhanced expression of ANO1 in head and neck squamous cell carcinoma causes cell migration and correlates with poor prognosis. *PLoS ONE*. 2012;7(8):e43265.

24. Kraus A, Peters DJM, Klanke B, et al. HIF-1alpha promotes cyst progression in a mouse model of autosomal dominant polycystic kidney disease. *Kidney Int*. 2018;94(5):887-899.

25. Schreiber R, Uliyakina I, Kongsuphol P, et al. Expression and function of epithelial anoctamins. *J Biol Chem*. 2010;285(10):7838-7845.

26. Magayr TA, Song X, Streets AJ, et al. Global microRNA profiling in human urinary exosomes reveals novel disease biomarkers and cellular pathways for autosomal dominant polycystic kidney disease. *Kidney Int*. 2020;98(2):420-435.

27. Benedetto R, Ousingsawat J, Wanitchakool P, et al. Epithelial chloride transport by CFTR requires TMEM16A. *Sci Rep*. 2017;7(1):12397.

28. Kraus A, Grampp S, Goppelt-Struebe M, et al. P2Y2R is a direct target of HIF-1alpha and mediates secretion-dependent cyst growth of renal cyst-forming epithelial cells. *Purinergic Signal*. 2016;12(4):687-695.

29. Cabrita I, Buchholz B, Schreiber R, Kunzelmann K. TMEM16A drives renal cyst growth by augmenting Ca^{2+} signaling in M1 cells. *J Mol Med*. 2020;98(5):659-671.

30. Viau A, Kotsis F, Boehlke C, et al. Divergent function of polycystin 1 and polycystin 2 in cell size regulation. *Biochem Biophys Res Comm*. 2020;521(2):290-295.

31. Yanda MK, Cha B, Cebotaru CV, Cebotaru L. Pharmacological reversal of renal cysts from secretion to absorption suggests a potential therapeutic strategy for managing autosomal dominant polycystic kidney disease. *J Biol Chem*. 2019;294(45):17090-17104.

32. Schwiebert EM, Wallace DP, Braunstein GM, et al. Autocrine extracellular purinergic signaling in epithelial cells derived from polycystic kidneys. *Am J Physiol Renal Physiol*. 2002;282(4):F763-F775.

33. Buchholz B, Teschemacher B, Schley G, Schillers H, Eckardt KU. Formation of cysts by principal-like MDCK cells depends on the synergy of cAMP- and ATP-mediated fluid secretion. *J Mol Med*. 2011;89(3):251-261.

34. Lérias J, Pinto M, Benedetto R, et al. Compartmentalized crosstalk of CFTR and TMEM16A (ANO1) through EPAC1 and ADCY1. *Cell Signal*. 2018;44:10-19.

35. Benedetto R, Ousingsawat J, Cabrita I, et al. Plasma membrane-localized TMEM16 proteins are indispensable for expression of CFTR. *J Mol Med*. 2019;97(5):711-722.

36. Duvvuri U, Shiwarski DJ, Xiao D, et al. TMEM16A induces MAPK and contributes directly to tumorigenesis and cancer progression. *Cancer Res*. 2012;72(13):3270-3281.

37. Zhang C, Balbo B, Ma M, et al. Cyclin-dependent kinase 1 activity is a driver of cyst growth in polycystic kidney disease. *J Am Soc Nephrol*. 2020;32(1):41-51.

38. Buchholz B, Schley G, Faria D, et al. Hypoxia-inducible factor-1alpha causes renal cyst expansion through calcium-activated chloride secretion. *J Am Soc Nephrol*. 2014;25(3):465-474.

39. Guilbault C, Saeed Z, Downey GP, Radzioch D. Cystic fibrosis mouse models. *Am J Respir Cell Mol Biol*. 2007;36(1):1-7.

40. Snouwaert JN, Brigman KK, Latour AM, et al. An animal model for cystic fibrosis made by gene targeting. *Science*. 1992;257(5073):1083-1088.

41. Clarke LL, Grubb BR, Gabriel SE, Smithies O, Koller BH, Boucher RC. Defective epithelial chloride transport in a gene-targeted mouse model of cystic fibrosis. *Science*. 1992;257(5073):1125-1128.

42. Berg P, Svendsen SL, Sorensen MV, et al. Impaired renal HCO(3) (-) excretion in cystic fibrosis. *J Am Soc Nephrol*. 2020;31(8):1711-1727.

SUPPORTING INFORMATION

Additional supporting information may be found online in the Supporting Information section.

> **How to cite this article:** Talbi K, Cabrita I, Kraus A, et al. The chloride channel CFTR is not required for cyst growth in an ADPKD mouse model. *FASEB J*. 2021;35:e21897. https://doi.org/10.1096/fj.202100843R